Optics and Photonics

1 Dispersion Managed Solitons and Polarization Mode Dispersion

Sponsor

US Air Force Office of Scientific Research
Grant F4920-98-1-0139

Project Staff

Professor Hermann A. Haus, Dr. Yijiang Chen, John Fini

We have begun work on dispersion managed solitons for long distance propagation. In dispersion management, the fiber is spliced from segments with group velocity dispersions of opposite sign. This is presently a very active field of research, since the performance of dispersion managed solitons is superior to that of solitons propagating on a uniform fiber.[1-3]

Communication systems utilizing dispersion managed solitons, still may not be deployed in spite of their excellent potential performance, because "linear propagation" using wavelength multiplexing has made enormous progress. However, bit-rates in individual channels are pushed upward, 40 Gb/s being under development. At high bit-rates, polarization mode dispersion (PMD) affects linear propagation adversely, putting a limit on the maximum transmissible bit-rate. PMD is caused by the unavoidable group velocity birefringence (two orthogonal polarizations travel at different group velocities). The principal polarizations vary randomly along the fiber. We have studied the effect of first order PMD on solitons and dispersion managed solitons and found that they display superior characteristics with regard to PMD. PMD excites internal oscillations of the soliton. The relative positions and the relative carrier frequency displacements of the two orthogonal polarizations behave like the position and momentum of a noise drive harmonic oscillator. The oscillations build up to a maximum level when the rate of excitation equals the rate of loss due to radiation (via the continuum). The soliton breaks up when the relative displacement approaches the width of the soliton. This puts an upper limit on the permissible PMD. This upper limit is independent of the bit-rate, unlike the case of linear propagation.

The rate of energy supply to the continuum by PMD is constant. Eventually, the level of the continuum would build up to affect the bit-error rate. However, the spectrum of the continuum excited PMD is zero at the carrier frequency and broader than the spectrum of the soliton. Filters can prevent the build-up of the continuum.

It follows from this scenario that solitons can overcome first order PMD at any bit-rate and for any distance, provided the PMD is below a certain threshold value. Second order PMD becomes important when the frequency dependence of the group velocity birefringence cannot be ignored. It can be shown that any fiber with first order PMD naturally possesses second order PMD, even if individual segments of the fiber do not possess group velocity dispersion (frequency dependence of group velocity. Second order PMD causes continuum generation over and above that of first order PMD. Again, filtering can keep it under control.

References

1 Y. Chen and H.A. Haus, "Dispersion-Managed Solitons with Net Positive Dispersion," *Opt. Lett*. 23: 1013-1015 (1998).

2 Y. Chen and H.A. Haus, "Dispersion-managed Solitons in the Net Positive Dispersion Regime," *J. Opt. Soc. Am. B* 16: 24-30 (1999).

3 Y. Chen and H.A. Haus,"Collisions in Dispersion-Managed Soliton Propagation," *Opt. Lett*. 24: 217-219 (1999).

Publications

Chen, Y., and H.A. Haus, "Dispersion-Managed Solitons with Net Positive Dispersion." *Opt. Lett.* 23: 1013-1015 (1998).

Chen, Y., and H.A. Haus, "Dispersion-Managed Solitons in the Net Positive Dispersion Regime." *J. Opt. Soc. Am. B* 16: 24-30 (1999).

Chen, Y., and H.A. Haus, "Collisions in Dispersion-Managed Soliton Propagation," *Opt. Lett*. 24: 217-219 (1999).

Haus, H.A., and Y. Chen, "Perturbation of Manakov Solitons." Submitted to *Phys. Rev. A*.

Chen, Y., and H.A. Haus, "Solitons and Polarization Mode Dispersion, *Opt. Lett.* Forthcoming.

Chen, Y, and H.A. Haus, "Manakov Solitons and Polarization Mode Dispersion, *Chaos.* Forthcoming.

Fini, J., and H.A. Haus, *Second Order PMD Produced by First Order PMD*, Quantum Optics Memo 93, (Cambridge: MIT Research Laboratory of Electronics, 1999), to be submitted for publication

2 Noise Figure of Optical Amplifiers

Sponsor

Air Force Office of Scientific Research (Defense Advanced Research Projects Agency)
Grant F49620-96-0126

Project Staff

Professor Hermann A. Haus

The noise figure definition currently used for the characterization of the noise performance of optical amplifiers[1] is in conflict with the IEEE standard definition developed for amplifiers in the LF, UHF, VHF and microwave regime.[2] The IEEE noise figure is defined as the ratio of input and output signal-to-noise ratios (SNR's), where the SNR is defined as the ratio of signal power and noise power. . The noise figure of a linear amplifier is signal level independent. This noise figure definition addresses specifically linear amplifiers, since the signal level is necessarily low and the amplifier behaves linearly when SNR considerations enter the characterization. The transfer function of the amplifier is independent of the signal level. The noise figure of a cascade of amplifiers obeys the standard cascading formula.[2]

Optical fiber amplifiers are also linear amplifiers of the electromagnetic field. The signal may saturate the gain; yet, because of the long relaxation time of the gain medium, inter-symbol interference does not occur. The amplifier still operates as a linear amplifier of reduced gain. Yet, the noise figure definition in current use is defined as the ratio of SNR's at input and output, when ideal photo-detectors are imagined to measure the input and output. The SNR's are defined in terms of mean square photon (or photo-electron) number and mean square photon number fluctuations.[2] The noise figure thus defined is a function of the signal level. It does not obey the standard cascading formula.[3]

Two alternate definitions of noise figure that are extensions of the noise figure definition for linear amplifiers have been proposed in Ref. [3]. Both provide the same information. Both obey the cascading formula.

In the meantime, another cogent reason has been found that argue against the noise figure definition currently used. Radio astronomy utilizes wavelength from microwaves to the visible. This requires a self consistent noise figure definition that covers the entire range of wavelengths. We have shown that the two noise figure definitions of reference 3 can be generalized to accomplish this. Further, we have shown that the information provided by the measurement of noise figure and gain is sufficient to describe the statistics of the field distribution (Gaussian) and of the photons or photo-electrons. These aspects of the proposed noise figure definitions, we believe, argue in favor of their adoption.

References

1 H.A. Haus, "Subcommittee 7.9 on Noise, Chairman, IRE standards on Methods of Measuring Noise in Linear Two-ports. 1959," *Proc. IRE* 48: 60-74 (1960).

2 E. Desurvire, *Erbium Doped Fiber Amplifiers; Principles and Applications* (New York: Wiley, 1994).

3 H.A. Haus, "The Noise Figure of Optical Amplifiers," *Photonics Technol. Lett.* 10: 1602-1604 (1998), Erratum 11: 143 (1999).

4 H.A. Haus, "Noise Figure Definition Valid from RF to Optical Frequencies," *IEEE J. Selected Topics Quantum Electron*., forthcoming.

Publications

Haus, H.A., "The Noise Figure of Optical Amplifiers," *IEEE Photonics Technol. Lett.* 10: 1602-04 (1998); Erratum 11: 143 (1999).

Haus, H.A., "Noise Figure Definition Valid from RF to Optical Frequencies," *IEEE J. Sel. Topics Quantum Electron.* Forthcoming.

3 Quantum Noise of Mode-locked Lasers

Sponsor

Air Force Office of Scientific Research (Defense Advanced Research Projects Agency)
Grant F49620-96-0126
Office of Naval Research
Grant N00014-92-J-1302

Project Staff

Professor Hermann A. Haus, Charles X. Yu, Mathew Grein

Passively mode-locked fiber lasers have an unusually small pulse-timing jitter.[1,2] The pulse-stream can provide accurate time delays for sampling applications. There is particular interest in the application to broadband A to D converters which need accurate sampling.

This is the motivation for the determination of the ultimate lower limit on the timing jitter set by quantum noise. We have developed a fully quantum mechanical analysis of the noise in passively mode-locked solid state lasers. Each gain or loss element within the laser is a source

of quantum noise (zero point fluctuations). A filter with frequency dependent loss also contributes noise. This noise is fundamental and unavoidable and sets a lower limit on the noise of the system. If the system emits soliton-like pulses, the pulses have four degrees of freedom: amplitude, phase, position and momentum. All of these are noise driven and fluctuate. Their fluctuations have been evaluated. It is of interest to note that the fluctuations inside the laser are different from those that would be derived from a semi-classical theory (signal plus additive noise power). On the other hand, the fluctuations of the emitted pulses outside the laser derived from quantum theory check with the predictions of the semi-classical theory.

If the pulse-stream is to be timed, active mode-locking is necessary. We have developed the quantum theory of actively mode-locked lasers.[3] With an eye on semiconductor lasers, we have allowed for gain relaxation times comparable to the pulse width. Under these conditions, amplitude fluctuations translate into timing jitter. As a consequence, the timing jitter of semiconductor lasers is inherently larger than that of solid state or fiber lasers.

References

1 H.A. Haus, M. Margalit, and C. X. Yu, "Quantum Noise of Mode-locked Lasers," submitted to *J. Opt. Soc. Am. B.*

2 H.A. Haus and M. Grein, *Quantum Limit on Timing Jitter of Actively Mode-locked Lasers*, Quantum Optics Memo 93 (Cambridge: MIT Research Laboratory of Electronics, 1999).

Publications list

Haus, H.A., M. Margalit, and C. X. Yu, "Quantum Noise of Mode-locked Lasers," submitted to *J. Opt. Soc. Am. B.*

Haus, H.A., and M. Grein, *Quantum Limit on Timing Jitter of Actively Mode-locked Lasers*. Quantum Optics Memo 93. Cambridge: MIT Research Laboratory of Electronics, 1999.

4 A GHZ Regeneratively Synchronized Passively Modelocked Fiber Laser

Sponsor

Office of Naval Research
Grant N00014-92-J-1302

Project Staff

Charles X. Yu, Professor Hermann A. Haus, Professor Erich P. Ippen

Wavelength division multiplexing (WDM) multiplexes different wavelength channels on the same fiber to increase the capacity of the lightwave transmission system. As the number of channels increases in such a system, the number of transmitters increases as well if one transmitter is used for each channel. Thus a broadband pulsed laser that can provide many channels from a single source maybe a viable alternative.[4] In addition to being broadband, the laser source should have gigahertz (GHz) repetition rate(rep-rate) since the transmission speed is determined by the laser repetition rate, and be synchronizable to the system clock. Active modelocking incorporates a modulator in the laser cavity to provide GHz rep-rate and clock synchronization. However it only produces picosecond pulses even in the presence of pulse shortening mechanisms such as soliton effects.[5] Passive modelocking can provide broad bandwidth but the ones that do have low rep-rate.

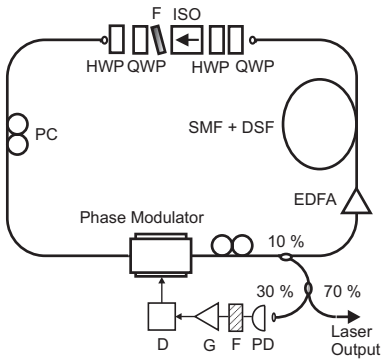

Figure 1. Laser Schematic, HWP: Half Wave Plate; QWP: Quarter Wave Plate; PC: Polarization Controller.

We add a modulator in a passively modelocked laser to achieve broad spectrum at GHz rep-rate and clock synchronization. The laser schematic is shown in Fig. 1. Part of the optical output is detected electronically and amplified to drive the phase modulator. The RF and the optical spectra of the output when the modulator is on are shown in Figs. 2a and 2b. The RF suppression is >60 dB and the spectral FWHM is 5.6 nm. Figures 2c and 2d show the RF and the optical spectra when the modulator is off. The absence of regenerative feedback leaves the pulses in random time slots (Fig 2c) but the envelope of the spectrum remains essentially unchanged (Fig. 2d). Thus passive modelocking shapes the pulses. The excellent RF suppression in Fig. 2a shows that the modulator synchronizes the pulses and prevents pulse dropouts. The pulsewidth is 480 fs and is shorter than what is possible via harmonic modelocking with solitonic shortening.[6] The amplitude and timing jitter of the laser are measured to be 0.03% and 86 fs, respectively. Figure 3 the shows the seventh harmonic of the laser. The jitter is low-frequency and mainly due to white noise. The inset shows the jitter's quadratic dependence on harmonics. We have developed a noise theory and the jitter can be accounted for when ASE is assumed to be the sole noise source.

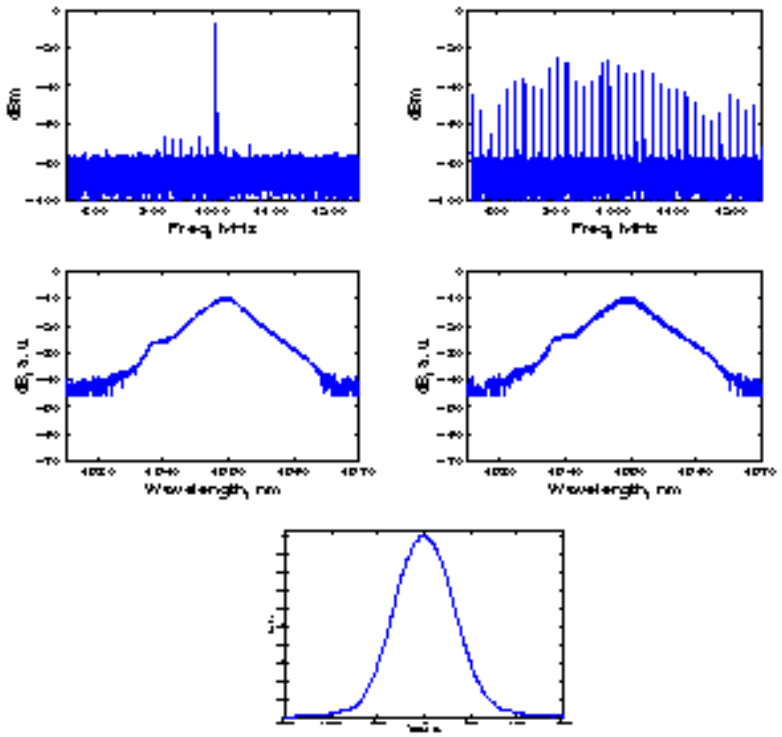

Figure 2. Output of the laser: a) RF spectrum b) optical spectrum when the modulator is on, c) RF spectrum d) optical spectrum when the modulator is off; e) Autocorrelation of the laser output when the modulator is on. The pulsewidth is 480 fs.

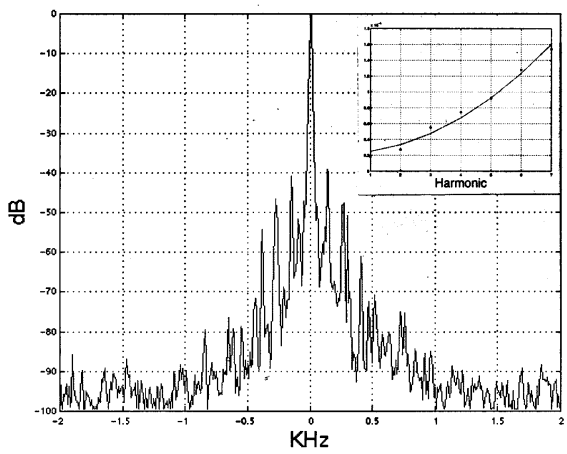

Figure 3. Harmonic seven (inset: quadratic jitter fitting).

References

1 T. Morioka, S. Kawanishi, K. Mori and M. Saruwatari, "Transform-Limited, fs WDM Pulse Generation by Spectral Filtering of Gigahertz Supercontinuum," *Electron. Lett*. 30: 1166 (1994).

2 T. Carruthers and I. N. Duling, "A 10-GHz, 1.3 ps erbium fiber laser employing soliton pulse shortening," *Opt. Lett*. 21: 1927 (1996).

3 F. X. Kärtner, D. Kopf, and U. Keller, “Solitary-pulse stabilization and shortening in actively modelocked lasers,” *J. Opt. Soc. Am. B* 12: 486 (1995).

5 Soliton Squeezing in Optical Fiber

Sponsor

Office of Naval Research
Grant N00014-92-J-1302

Project Staff

Charles X. Yu, Professor Hermann A. Haus, Professor Erich P. Ippen

Highly accurate optical phase measurement apparatuses such as the laser gyroscope are increasingly being deployed in many applications that require inertial navigation and platform stabilization. Many of these sensors use an interferometric arrangement to sense any motion. The accuracy of such high precision phase sensitive interferometric measurements is fast approaching the limits set by the shot noise, which originates from fluctuations of the vacuum field. It has been shown[1] that an interferometric phase measurement can achieve higher SNR than the standard quantum limit by using “squeezed” states. Squeezed quantum states of the electromagnetic field are states that have reduced fluctuations in one phase of the field at the expense of increased fluctuations in the quadrature phase. We have pursued the generation of squeezed states in fibers since their use in a measurement has to be accomplished with minimum loss. Single mode fibers and their interconnections can be made with very small insertion losses. We have been able to observe 5dB squeezing using pulses at 1.3 mm[3]. The squeezing is limited because different temporal portions of the Gaussian pulse do not interact with each other. Each portion experiences different nonlinearity depending on its amplitude and thus different amount of squeezing. The overall squeezing is an average over the entire pulse. Because of the low peak power in the pulse wings the overall squeezing cannot improve.

To overcome this limitation we will attempt squeezing at 1.55 mm. At 1.55 mm the fiber has negative dispersion and the pulses form solitons. The different temporal portions of an ideal soliton are correlated with each other and experiences the same squeezing. Thus no limit due to the pulse shape exists for soliton squeezing. Theoretical analysis indicates that greater than 20 dB squeezing is achievable before the Raman effect places a floor on the observable squeezing.

Past efforts to observe soliton squeezing has largely been frustrated by Guided Acoustic Wave Brillion Scattering(GAWBS)[7]. GAWBS is a phase noise generated in fiber due to the fiber's acoustic modes and cannot be cancelled via balanced detection. GAWBS usually has frequency content from 20 MHz to 1 GHz. To combat GAWBS we use a pulsed source whose repetition rate is greater than 1 GHz. Squeezing can then be observed between GAWBS spikes. We have achieved a 1 GHz fiber laser source using harmonic modelocking[2]. To reach the soliton condition we need ~150 mW in one single polarization. Such power is difficult to achieve directly from the laser or even from a conventional fiber amplifier. We have made a double-clad Er/Yb fiber amplifier with gain fiber denoted by Lucent Technologies. Greater than 1 Watt of saturated power has been obtained with this amplifier. We are optimizating this amplifier to achieve 2 Watts of saturation power stably. Amplification with the current amplifier configuration leads to pulse peak power in excess of 1 kW, more than sufficient for our squeezing experiments.

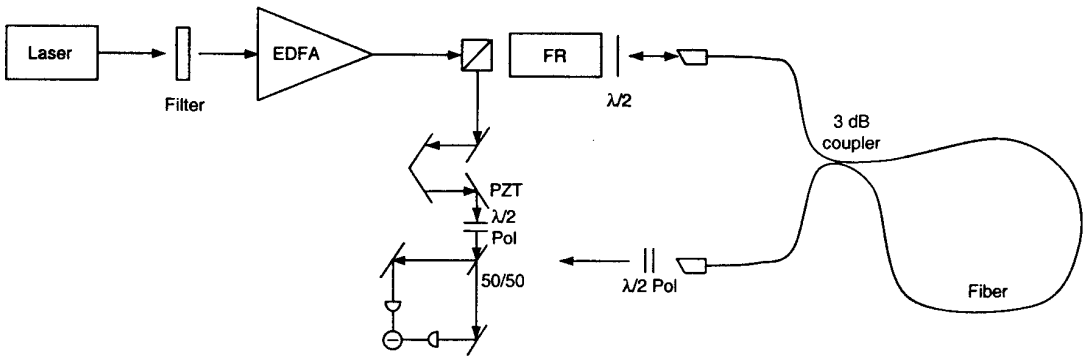

Figure 4. Experimental setup.

The amplified output is sent into a balanced sagnac loop mirror[3]. The schematic is shown in Fig. 4. The input is reflected back towards the amplifier but the circulator separate it so that the it can be reused as the local oscillator (LO) for homodyne detection. The squeezed vacuum exits the vacuum port and meets the LO at the 50/50 beam splitter. The two beams are carefully matched in space, time and polarization. A balanced detector is used to cancel the classical noise of the LO. The noise of the amplified pulses are 18 dB above the shot noise for 5-10 MHz. Our balanced detector can cancel 27 dB of noise. We have also calibrated our detector with flashlights and verified the shot-noise levels. Thus our detector output is shot-noise limited for that frequency. Figure 5 shows the averaged normalized power spectrum at 10 MHz with and without the squeezed vacuum when the PZT is driven slowly with a sawtooth and 3 dB of squeezing has been observed. Because our interferometric setup is not stabilized, the phase between the LO and the squeezed vacuum slips and the averaged results show less squeezing than the actually amount. Though too noisy to be conclusive, single-shot spectra seem to suggest at least 5 dB squeezing. We are currently building a feedback stabilization circuit to observe this large squeezing.

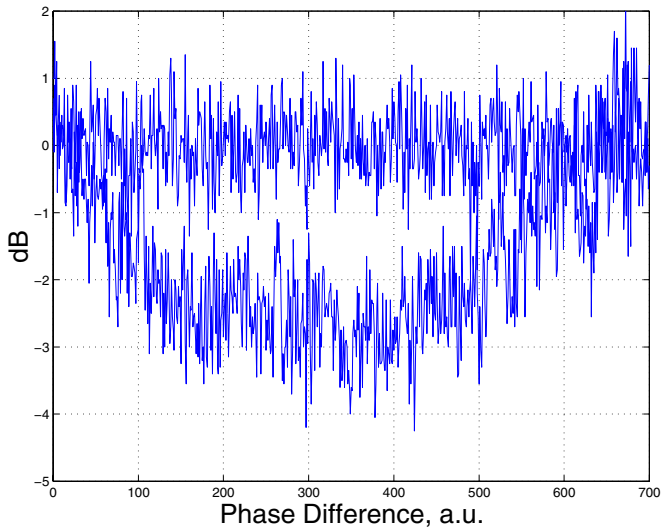

Figure 5. Squeezed spectrum and shot noise spectrum

References

1 C. Caves, "Quantum-Mechanical Noise in an Interferometer," *Phys. Rev. D* 23: 1693 (1981).

2 R. Shelby, M. Levenson, and P. Bayer, "Guided Acoustic-Wave Brillouin Scattering," *Phys. Rev. B* 31: 5244-5252 (1985).

3 M. Margalit, C. Yu, E.P. Ippen, and H.A. Haus, "Harmonic Mode-Locking using Regenerative Phase Modulation," *IEEE Photon. Technol. Lett*. 10: 337-339 (1998).

4 K. Bergman, H.A. Haus, E.P. Ippen, and M. Shirasaki, "Squeezing in a Fiber Interferometer with a GHz Pump," *Opt. Lett*. 19: 290 (1994).

6 High Density Optical Integration

Sponsor

Air Force Office of Scientific Research (MURI) Advanced Research Project Agency
Grant F49620-96-0216
MRSEC Program of the National Science Foundation
Award DMR 98-08941

Project Staff

Professor Hermann A. Haus, Christina Manolatou, Mohammed Jalal Khan

Our work is primarily concerned with the design and modelling of high index contrast photonic devices. These include resonant channel filters for use in wavelength division multiplexing (WDM), low-loss waveguide components for dense optical integration, and more recently mode transformers for efficient coupling of these devices with optical fibers. The common feature of these devices is that they are based on high- or low-Q resonant cavities and design principles borrowed from microwave engineering. Our theoretical approach starts with the coupled mode theory as a first estimate of the expected performance but due to the complexity of the structures numerical simulations are performed for an accurate calculation of the response and the field patterns. For our simulations we have been using the Finite Difference Time Domain (FDTD) mostly in two dimensions. Our simulations have shown the possibility of achieving very high-Q in high index-contrast optical resonators of polygonic shape, such as squares and triangles, by placing the nulls of the electric field of the resonant mode at the corners. We have used such resonators as building blocks in most of our designs. Thus, waveguide bends, crossings and splitters with excellent performance charactersistics have been demonstrated numerically using high index contrast waveguides and resonant cavities.[1] The idea is based on the fact that a lossless resonator with two ports and appropriate symmetry allows complete reflectionless transmission on resonance. In practice there is always some radiation loss from the resonator which must be counteracted by strong coupling to the waveguide mode.

This lowers the external Q of the resonator leading to a very broad bandwidth. We have applied this concept in 2D FDTD simulations of high index contrast waveguide components (3.2/1). By modifying the corner of a right angle bend into a resonant structure with symmetry we were able to achieve transmission over 98% with negligible reflection over a bandwidth of more than 100 nm. A strongly coupled pair of similar structures was used in a T- junction to achieve transmission over 49% in each arm. Figure 6 shows the electric field pattern in the T-junction. We have also looked at planar waveguide crossings where the intersection region was designed as a cavity supporting two orthogonal modes with a nodal plane along one of the two waveguide axes. Excitation of one mode from the input waveguide results in full transmission with no crosstalk into the intersecting waveguide.[1-2]

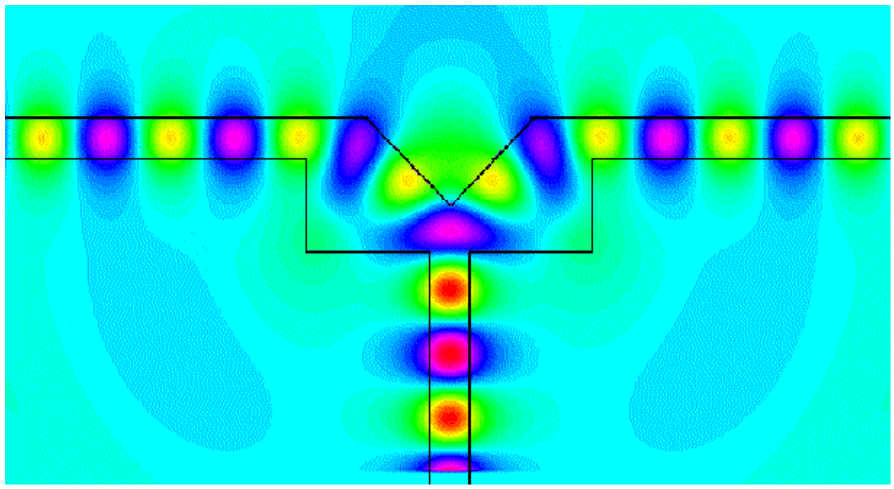

Figure 6. Electric field amplitude distribution in a low-loss T-junction.

Channel dropping filters employing one or more pairs of coupled square resonators of high-Q, placed between two waveguides have also been investigated as alternative to ring resonator filters.[3-4] The operation of this type of filter is based on the excitation of two degenerate symmetric and antisymmetric standing wave modes which is achieved if the mutual coupling between the two modes is counteracted by the indirect coupling via the waveguides. Our FDTD simulations have qualitatively verified the predictions of coupled mode theory but also revealed the sensitivity to the design parameters.

An important issue is the coupling of the above devices with optical fibers. The mode size of an optical fiber is several microns, much larger than the submicron width of our single mode high index-contrast waveguides. We have been investigating ways to improve the coupling efficiency using a resonant cavity or a cascade of cavities of decreasing size as mode transformers in combination with impedance matching techniques analogous to those used in microwave engineering. Our preliminary studies have given up to 70% coupling efficiency, with radiation between 10-20% and the rest back-reflection. An example of this structure and its wavelength response are shown in Fig. 7 (a) and (b), respectively. The radiation loss is the main problem in these structures. Further investigation of these resonant mode- transformers is currently in progress in order to improve their performance and arrive at a systematic design.

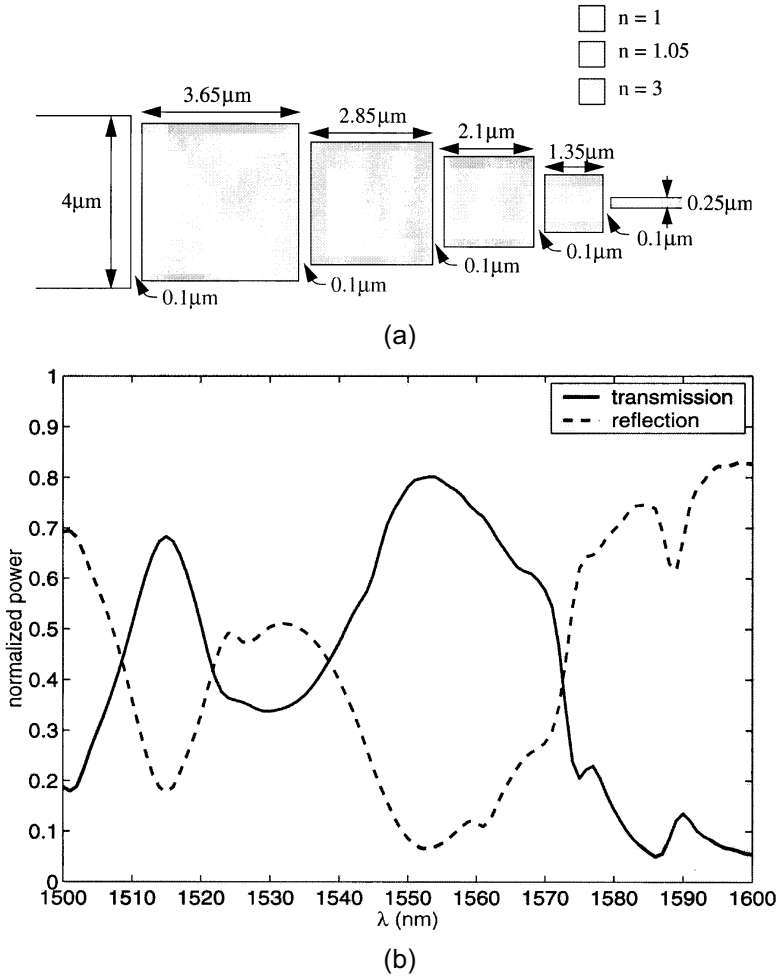

Figure 7. (a) Schematic mode transformer consisting of a cascade of square resonators for coupling between wide low-index waveguide and a submicron high index waveguide. (b) Associated wavelength response found by FDTD.

References

1 C. Manolatou, S.G. Johnson, S. Fan, P.R. Villeneuve, H.A. Haus, and J.D. Joannopoulos, ‘‘High Density Integrated Optics,’’ *J. Lightwave Technol*. 17(9): 1682-1692 (1999).

2 S.G. Johnson, C. Manolatou, S. Fan, P.R. Villeneuve, J.D. Joannopoulos, and H. A. Haus, ‘‘Elimination of Crosstalk in Waveguide Intersections,’’ *Opt. Lett*. 23(23): 1855-1857 (1998).

3 C. Manolatou, M.J. Khan, S. Fan, P.R. Villeneuve, H.A. Haus, and J.D. Joannopoulos, ‘‘Coupling of Modes Analysis of Resonant Channel Add/dop Filters,’’ *IEEE J. Quantum Electron*. 35(9): 1322-1331 (1999).

4 M.J. Khan, C. Manolatou, S. Fan, P.R. Villeneuve, H.A. Haus, and J.D. Joannopoulos, ‘‘Coupling of Modes Analysis of Multipole Symmetric Resonant Channel Add/drop Filters,’’ *IEEE J. Quantum Electron*. 35(10): 1451-1460 (1999).

Publications

Manolatou, C., S.G. Johnson, S. Fan, P.R. Villeneuve, H.A. Haus, and J.D. Joannopoulos, "High-Density Integrated Optics," *J. Lightwave Technol*. 17(9): 1682-92 (1999).

Manolatou, C., M.J. Khan, S. Fan, P.R. Villeneuve, H.A. Haus, and J.D. Joannopoulos, "Coupling of Modes Analysis of Resonant Channel Add-Drop Filters," *IEEE J. Quantum Electron.* 35(9): 1322-1331 (1999).

Khan, M.J., C. Manolatou, S. Fan, P.R. Villeneuve, H.A. Haus, and J.D. Joannopoulos, "Mode-Coupling Analysis of Multipole Symmetric Resonant Add/Drop Filters," *IEEE J. Quantum Electron*. 35(10): 1451-60 (1999).

7 Channel Dropping Filter

Sponsor

Air Force Office of Scientific Research (MURI) Advanced Research Project Agency
Grant F49620-96-0216
MRSEC Program of the National Science Foundation
Award DMR 98-08941

Project Staff

Professor Hermann A. Haus, Christina Manolatou, Mohammed Jalal Khan

Wavelength division multiplexing has become the de facto method of increasing bandwidth of existing fiber optic networks. WDM involves multiplexing 12 independent channels, modulated with their own data, on to a single fiber thereby giving an n-fold increase in throughput of data. Whereas most WDM systems to date are simple point-to-point links, in which all the constituent channels are multiplexed at the transmitting point and then separated at the receiving point, there is a trend towards more sophisticated architecture consisting of multiple interconnected nodes. At each node one or more channel may be added or dropped allowing networks architects more flexibility in designing systems. A key component needed for WDM networks is the Add/Drop filter. We have been pursuing the design and construction of an integrated channel-dropping filter (CDF) which allows a single wavelength channel to be extracted from a multi-channel bus without disrupting any of the remaining channels. Over the past year considerable progress has been made in the fabrication process[1], our ability to compensate for fabrication errors and a more complete modelling of CDFs

[1] For fabrication update please see "development of Febrication Techniques for Building Integrated-Optical Grating-Based Filters" in this RLE Progress Report.

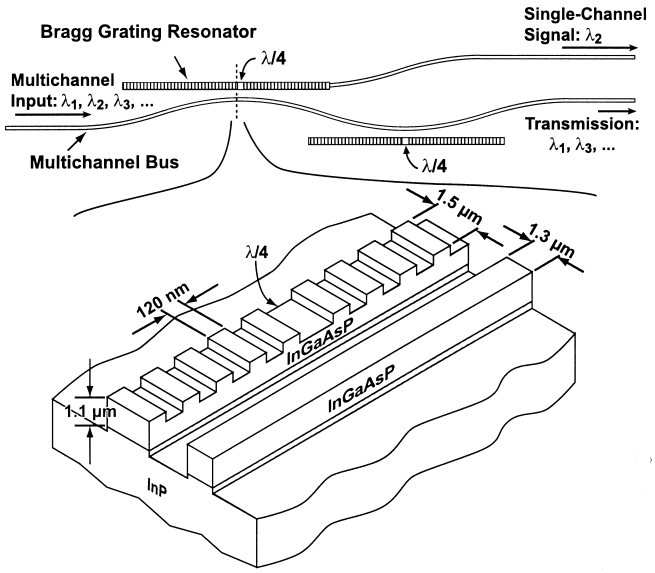

Figure 8. Schematic of channel dropping filter

Figure 8 shows a schematic of the CDF. The key component of the CDF is the quarter-wave shifted Bragg grating resonator which couples to the bus guide. Resonant excitation of the grating structure enables extraction of the desired channel. To address the complex design challenges of the CDF, we have developed an equivalent-circuit model that maps the Bragg grating based waveguides onto equivalent electrical circuits consisting of resistors, inductors, and capacitors. Once this association has been made, the spectral response of the filter may be engineered using standard circuit tables. For example, we have used the equivalent circuit technique to design third order Butterworth filters. Once we have mapped the electrical parameters to their corresponding optical parameters, we use computer simulations to calculate the physical dimensions of the waveguides and gratings that yield the desired values for these optical parameters. A more comprehensive circuit model which takes into account the spurious excitation of the Bragg resonator by a symmetric excitation is currently being explored. The resulting enhanced equivalent circuit model should yield better modeling of the CDF.

A dual approach of using analytic techniques and computer simulations to design devices enables us to generate detailed design tables which take into account and allow for unpredictable variations in the manufacturing sequence. One such variation is the change in the duty cycle from its design value during fabrication. The duty cycle of the grating is defined as the ratio of the grating tooth to the grating gap. For our design, we have chosen the duty cycle of the grating to be 50 %. However, in practice it is very difficult to hit this specification exactly and variations of 10% can be expected.. Any variation in duty cycle affects the optical parameter; the grating strength, the coupling between the resonator and bus guide and most importantly the requirement that the propagation constants of the bus and resonator guide are nominally identical. Without the ability to compensate for such variations the performance of the device could deteriorate significantly if the changes in duty cycle were large. However, by varying the grating depth and if needed the etch depth of the waveguides it is possible to restore the device performance. Table 1 shows how various optical parameters scale with the duty-cycle and the grating etch depth. It was generated by simulating the fields in different waveguide structures. An accurate measure of the duty-cycle can be obtained during the fabrication process and once it is known the tables can be used to determine the grating etch depth to achieve the desired optical parameters and device performance. A similar approach also allows us to compensate for variations in the composition of the core material, InGaAsP, across the wafer.

Grating Strength κ (cm^{-1})		Grating Depth (μm)				
		0.2	0.22	0.24	0.26	0.28
Duty Cycle	0.52	58.20	64.43	70.82	77.38	83.78
	0.54	58.32	64.69	71.05	77.63	84.17
	0.55	58.22	64.68	71.07	77.61	84.25
	0.56	58.20	64.59	71.05	77.57	84.34
	0.58	57.85	64.25	70.68	77.35	83.93

Propagation Constant Difference Δβ (cm^{-1})		Grating Depth (μm)				
		0.2	0.22	0.24	0.26	0.28
Duty Cycle	0.52	1.78	12.82	24.42	36.57	48.32
	0.54	-2.02	8.89	19.80	31.35	42.88
	0.55	-4.15	6.82	17.56	28.78	40.26
	0.56	-5.71	4.75	15.40	26.29	37.89
	0.58	-9.33	0.74	10.87	21.73	32.27

Coupling Strength μ (cm^{-1})		Grating Depth (μm)				
		0.2	0.22	0.24	0.26	0.28
Duty Cycle	0.52	9.91	10.35	10.76	11.16	11.70
	0.54	9.80	10.17	10.60	11.01	11.49
	0.55	9.79	10.06	10.48	10.88	11.26
	0.56	9.68	10.03	10.43	10.86	11.23
	0.58	9.56	9.89	10.28	10.62	11.06

Table 1.

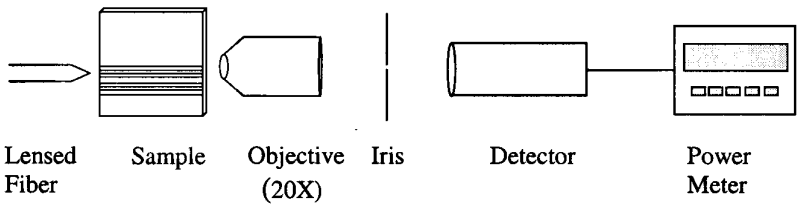

Figure 9. Setup for measurement of loss and index.

Measurements of loss and effective index were also performed on some preliminary waveguide devices that were fabricated. The measurement setup shown in Fig. 9 involved coupling light into the cleaved waveguide samples mounted on a tab using a lensed fiber. The light from the output facet of the waveguide was imaged onto an infrared camera to confirm that a guided mode was being observed. The infrared camera was then replaced by a power meter, which allowed power throughput measurement to be performed. By using a cutback technique the loss of the guides was estimated. Fabry-Perot scans of the sample were also taken. The free spectral range (FSR) allowed an estimate of the effective index. By measuring the modulation depth of the Fabry-Perot scan, the loss of the guides was estimated.

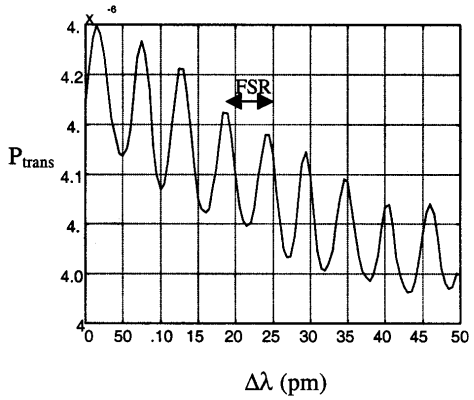

Figure 10. Transmitted power as indicator of loss and index.

8 Microsphere Resonators

Sponsor

Charles S. Draper Laboratory

Project Staff

Dr. Brent E. Little, Juha-Pekka J.V. Laine, Professor Hermann A. Haus

Silica microsphere whispering-gallery-mode resonators exhibit Q factors of over 10^{10}.[1] If successfully harnessed, such enormous Q's could prompt technological breakthroughs in a variety of fields ranging from high-resolution sensing to cavity QED-experimentation.[2-4] Within this context, RLE-Draper microsphere research targets the remaining obstacles to the practical utility of the resonators, as well as identifies and prototypes new application concepts.

The most important innovation to date is the successful employment of the Stripline-Pedestal Anti-Resonant Reflecting Optical Waveguide (SPARROW). This device represents the first generation of planar-waveguide couplers for sphere mode excitation. The primary advantage of the invention is that it facilitates the integration of high-Q microsphere cavities onto IO-circuits, creating novel opportunities especially in dynamic sensing applications. The SPARROW concept is based on eliminating sphere and guide mode leakage into the planar substrate by isolating the guide core with a high-reflectivity stack of silica and silicon layers. SPARROW coupling performance is demonstrated in Fig.11.

Other developments include theoretical whispering-gallery modeling of sphere performance in diverse coupling environments, higher-order mode mapping, and experimental demonstration of an accelerometer and a narrow-band add-drop filter. The accelerometer consists of a microsphere suspended above a SPARROW guide, with the sphere's stem serving both as the attachment point to the coupler chip and as the flexure arm providing force response, Fig. 12. Acceleration is measured by tracking extremely small changes in the coupling gap via whispering-gallery mode frequency shift and Q-charge. The add-drop filter SPARROW chip incorporates two parallel waveguides placed just outside field overlap, and a microsphere power transfer node sitting above the waveguides. Power is transferred from the input waveguide into the sphere and from it into the adjacent drop guide. Transfer efficiencies of up to 80% can be maintained with a Q of 10^6.

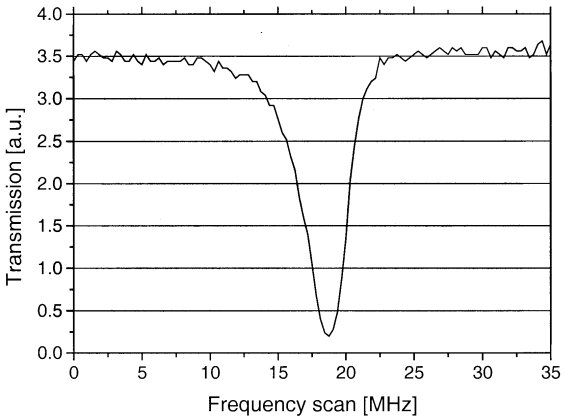

Figure 11. SPARROW transmission plot of a microsphere TE-resonance in the 1.55 μm region. A power transfer efficiency of over 95% and a Q-value of 0.5×10^8 is obtained for a sphere of diameter 220 μm, as coupled to an 8 μm wide waveguide.

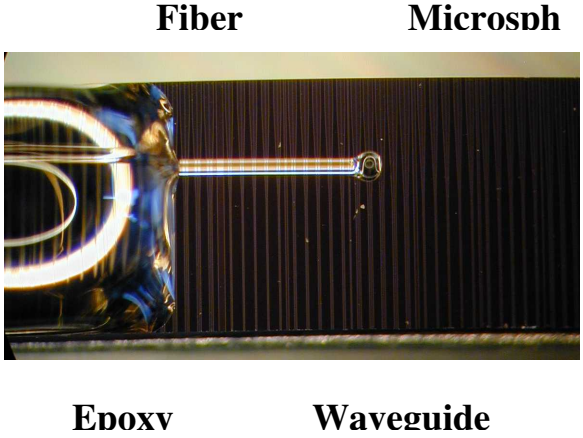

Figure 12. Prototype of the microsphere-based accelerometer. Sphere diameter 260 μm. Response of the fiber stem flexure is tracked by monitoring the corresponding changes in the whispering-gallery mode resonance characteristics. High sensitivity and dynamic range can be attained.

References

1 L. Collot, V. Lefevre-Seguin, M. Brune, J.M. Raimond, and S. Haroche, "Very High-Q Whispering Gallery Mode Resonances Observed on Fused Silica Microspheres," *Europhys. Lett.*, 23(5): 327-34 (1993).

2 B.E. Little, S. T. Chu, and H. A. Haus, "Track Changing by Use of the Phase Response of Microspheres and Resonators," *Opt. Lett.* 23(12): 894-96 (1998).

3 F. Treussart, N. Dubreuil, J. Knight, V. Sandoghdar, J. Hare, V. Lefevre-Seguin, J. M. Raimond, and S. Haroche, "Microlasers Based on Silica Microspheres," *Ann. Telecommun.* 52(11-12): 557-68 (1997).

4 A.B. Matsko, S.P. Vyatchanin, H. Mabuchi, and H.J. Kimble, "Quantum Nondemolition Detection of Single Photons in an Open Resonator by Atomic Beam Deflection," *Phys. Lett. A.* 192(2-4): 175-79 (1994).

Publications

Laine, J.-P., B. E. Little, and H. A. Haus, “Etch-eroded Fiber Coupler for Whispering- gallery-Mode Excitation in High-Q Silica Microspheres,” *IEEE Photonics Tech. Lett.* 11(11): 1429-30 (1999).

Little, B.E., J.-P. Laine, D. Lim, H. A. Haus, L. C. Kimerling, and S. T. Chu, “Pedestal Antiresonant Reflecting Waveguides for Robust Coupling to Microsphere Resonators and for Microphotonic Circuits,” *Opt. Lett*. 25(1): 73-75 (2000).